Please use this PDF proof to check the layout of your article. If you would like any changes to be made to the layout, you can leave instructions in the online proofing interface. First, return to the online proofing interface by clicking "Edit" at the top page, then insert a Comment in the relevant location. Making your changes directly in the online proofing interface is the quickest, easiest way to correct and submit your proof.

Please note that changes made to the article in the online proofing interface will be added to the article before publication, but are not reflected in this PDF proof.

Green Chemical Engineering xxx (xxxx) xxx

Contents lists available at ScienceDirect

Green Chemical Engineering

journal homepage: www.keaipublishing.com/en/journals/green-chemical-engineering

Original Article

Constructing D-π-A-π dye to obtain red-emission fluorescent probe for structured illumination microscopy imaging of lipid droplet dynamics

Wenchao Jiang [a,b], Jie Chen [a,b], Kai An [a,b], Pengjun Bao [a,b], Qinglong Qiao [a,***], Xiaogang Liu [c,**], Zhaochao Xu [a,*]

[a] CAS Key Laboratory of a CAS Key Laboratory of Separation Science for Analytical Chemistry, Dalian Institute of Chemical Physics, Chinese Academy of Sciences, Dalian, 116023, China
[b] University of Chinese Academy of Sciences, Beijing, 100049, China
[c] Fluorescence Research Group, Singapore University of Technologyand Design, 8 Somapah Road, Singapore, 487372, Singapore

HIGHLIGHTS

- A red-emission fluorescent probe for lipid droplets was developed.
- A strategy of D-π-A-π to modify the dye conjugation to get red-shifted emission.
- Lipid droplets dynamics in living cells were monitored with super-resolution imaging.
- Multiple consecutive fusions and fusions in a centrosymmetric manner of LDs were observed.

GRAPHICAL ABSTRACT

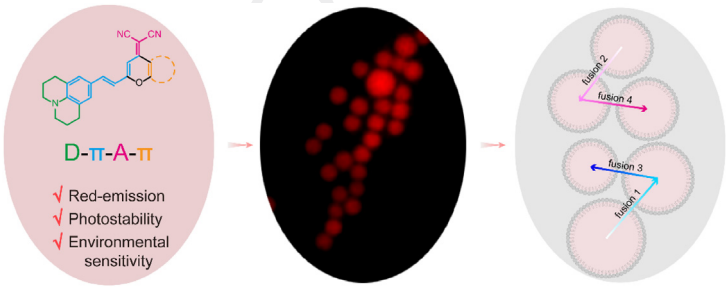

ARTICLE INFO

Keywords:
Lipid droplets
Fluorescent probe
Red-emission
D-π-A-π
Super-resolution imaging

ABSTRACT

Lipid droplets (LDs) are dynamic organelles interacting with a variety of intracellular organelles. Tracking intracellular LD dynamics employing synthetic small molecules is crucial for biological studies. Fluorescence imaging in the red and near infrared (NIR) region is more suitable for biological imaging due to its low phototoxicity and high signal-to-noise ratio. However, available LD-dyes in the red region with remarkable environmental sensitivity, selectivity for LDs staining are limited. Here, we constructed a red-emission D-π-A-π type LD-dye LD 688P with higher environmental sensitivity and suitable "calculated log P" (Clog P) for LDs dynamic imaging. LD 688P was proved to be highly selective and photostable for tracing LD fusion including multiple consecutive fusions and fusions in a centrosymmetric manner by super-resolution microscopy. We believe that the D-π-A-π skeleton would be an efficient strategy to construct red and even NIR-emission dyes.

Lipid droplets have important roles in lipid metabolism and storage, as well as membrane transport, protein degradation, and signal transduction [1–3]. They have a distinctive structure composed of phospholipid monolayer decorated with proteins and a hydrophobic core containing neutral lipids such as triacylglycerols (TAGs) and cholesteryl esters [4]. LDs are thought to originate from the endoplasmic reticulum,

* Corresponding author.
** Corresponding author.
*** Corresponding author.
E-mail addresses: qqlqiao@dicp.ac.cn (Q. Qiao), xiaogang_liu@sutd.edu.sg (X. Liu), zcxu@dicp.ac.cn (Z. Xu).

https://doi.org/10.1016/j.gce.2022.07.002
Received 27 May 2022; Received in revised form 23 June 2022; Accepted 7 July 2022
Available online xxxx

Please cite this article as: W. Jiang et al., Constructing D-π-A-π dye to obtain red-emission fluorescent probe for structured illumination microscopy imaging of lipid droplet dynamics, Green Chemical Engineering, https://doi.org/10.1016/j.gce.2022.07.002

and after generation, are transported to the cytoplasm and grow up *via* fusion of LDs or combining with neutral lipids other than LDs. They are highly dynamic and interact with various intracellular organelles, including ER, mitochondria, lysosomes, and nucleus [5–8]. Growing research suggested LDs were relative to many metabolic disorders such as fatty liver, arteriosclerosis, and even cancer [6,9]. Therefore, monitoring lipid droplet number, size, morphology as well as dynamic processes is crucial for the understanding and treatment of related diseases.

To realize the real-time observation of LDs *in situ* and study their versatile physiological functions [10,11], fluorescence imaging, especially structured illumination microscopy (SIM) imaging, provides a powerful approach with high spatial-temporal resolution [12,13]. LDs are highly heterogeneous organelles, that vary in number, size as well as composition. They are very different in diverse kinds of cells, or even within the same cell [14], which requires LD probes with high brightness and excellent selectivity for precise staining of even tiny nascent LDs [15]. Moreover, LDs show high dynamics inside the cells. Realizing long-term observation of LDs dynamics and their interaction with various organelles, high photostability, and multi-color LD probes are in high demand [16,17]. Especially for LD dyes in the red region which can reduce phototoxicity to biological samples and light scattering, and eliminate the interference of biological background fluorescence [18, 19], they proved susceptible to photobleaching and the types are limited yet [20–24].

Several methods have been developed to extend the wavelength of LD dyes (Fig. 1). Three LD dyes with different colors of Lipi-Blue, Lipi-Green, and Lipi-Red were obtained by varying the intensities of the electron-acceptor and electron-donor by Ueno and co-workers [25]. This method is dependent on the choice of donor and acceptor, and the targeting of the dye is not controllable. The other method to extend the dye wavelength was based on the expansion of the conjugation system. Klymchenko and co-workers expanded π-bridge of D-π-A by methine obtaining a series of dioxaborine-containing merocyanines which cover the visible spectrum and the near-infrared region [26]. Similarly, expanding π-bridge of D-π-A by aromatic ring also increases the dye wavelength [20,27–29] (Fig. 1). Nevertheless, these strategies significantly increase "calculated log *P*" (Clog *P*), which is not conducive to the stability of the molecules, the selectivity of staining, and achieving dynamic imaging of LDs. Systematic research has shown that reducing Clog *P* can effectively improve the stability of LD dyes [30]. Unfortunately, existing red LD probes cannot meet this requirement well.

In this paper, we reported a red-emission fluorescent probe LD 688P for LDs dynamic imaging based on a strategy of D-π-A-π to extend the dye conjugation system (Fig. 1). The commercial dye LD 688 has an appropriate Clog *P* but a short wavelength. In comparison with LD 688, LD 688P, in which the benzene ring was incorporated into one side of the acceptor, red-shifted the absorption and emission wavelengths by delocalization of electrons in the excited state, allowing the whole molecule to remain perfectly planar. A slight increase in the Clog *P* value was more conducive to the accumulation of LD 688P in LDs and improve the imaging signal-to-noise ratio [30]. LD 688P exhibited remarkable environmental sensitivity and photostability for LDs staining. By using SIM imaging, we monitored the fusion of LDs, including continuous LD fusion in a large cluster and an orderly LD fusion in a small cluster.

Firstly, LD 688P was synthesized according to the method reported in the literature [31] (Fig. S1). Then the UV–Vis absorption and fluorescence spectra of LD 688 and LD 688P were investigated in solvents with different polarities (Fig. 2a and S2, Tables S1 and S2). Compared with LD 688, LD 688P exhibited longer wavelengths both for maximum absorption and maximum emission. With increasing solvent polarity from chloroform to water, the absorption and emission of LD 688P red-shifted to a longer wavelength as a result of the intramolecular charge transfer (ICT) (Tables S1 and S2). A linear relationship between maximum emission wavelengths (λ_{em}) *vs.* the solvent polarity parameters (E_T (30)) both for LD 688 and LD 688P was observed (Fig. 2b), while LD 688P proved to be more environmentally sensitive due to its larger slope. It

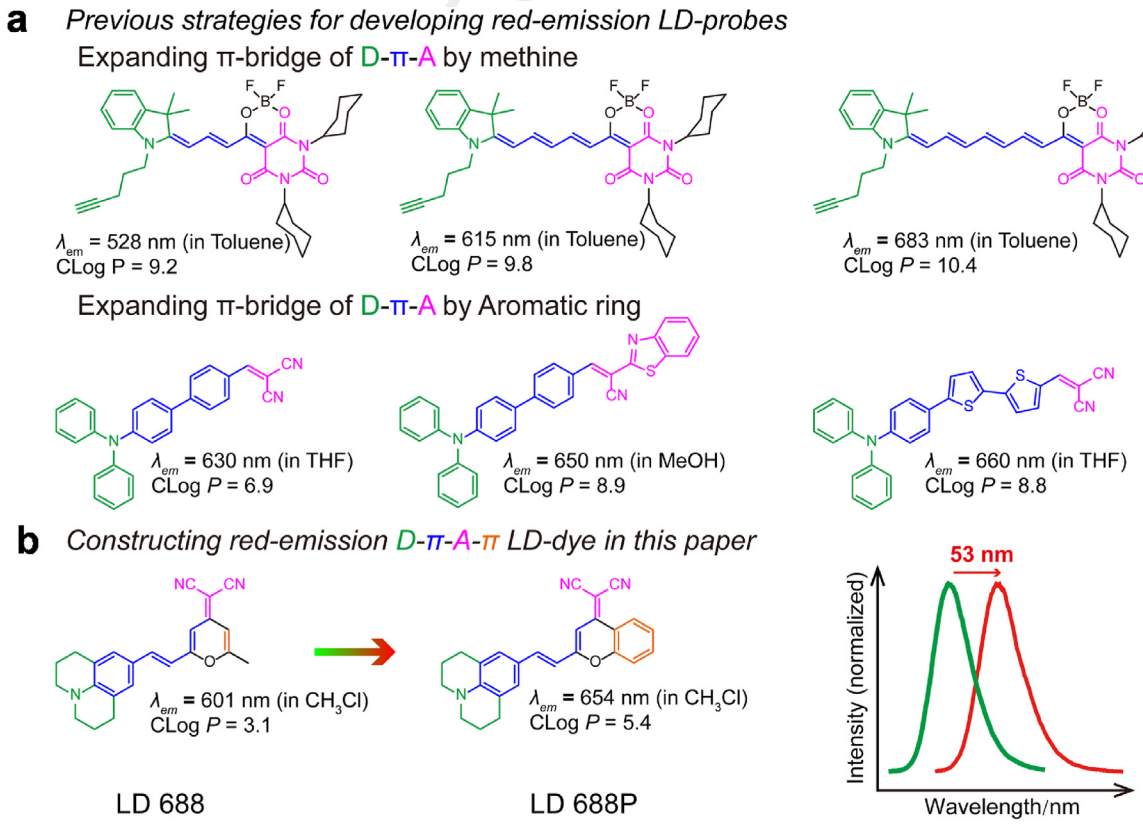

Fig. 1. Different strategies for developing red-emission LD-dyes.

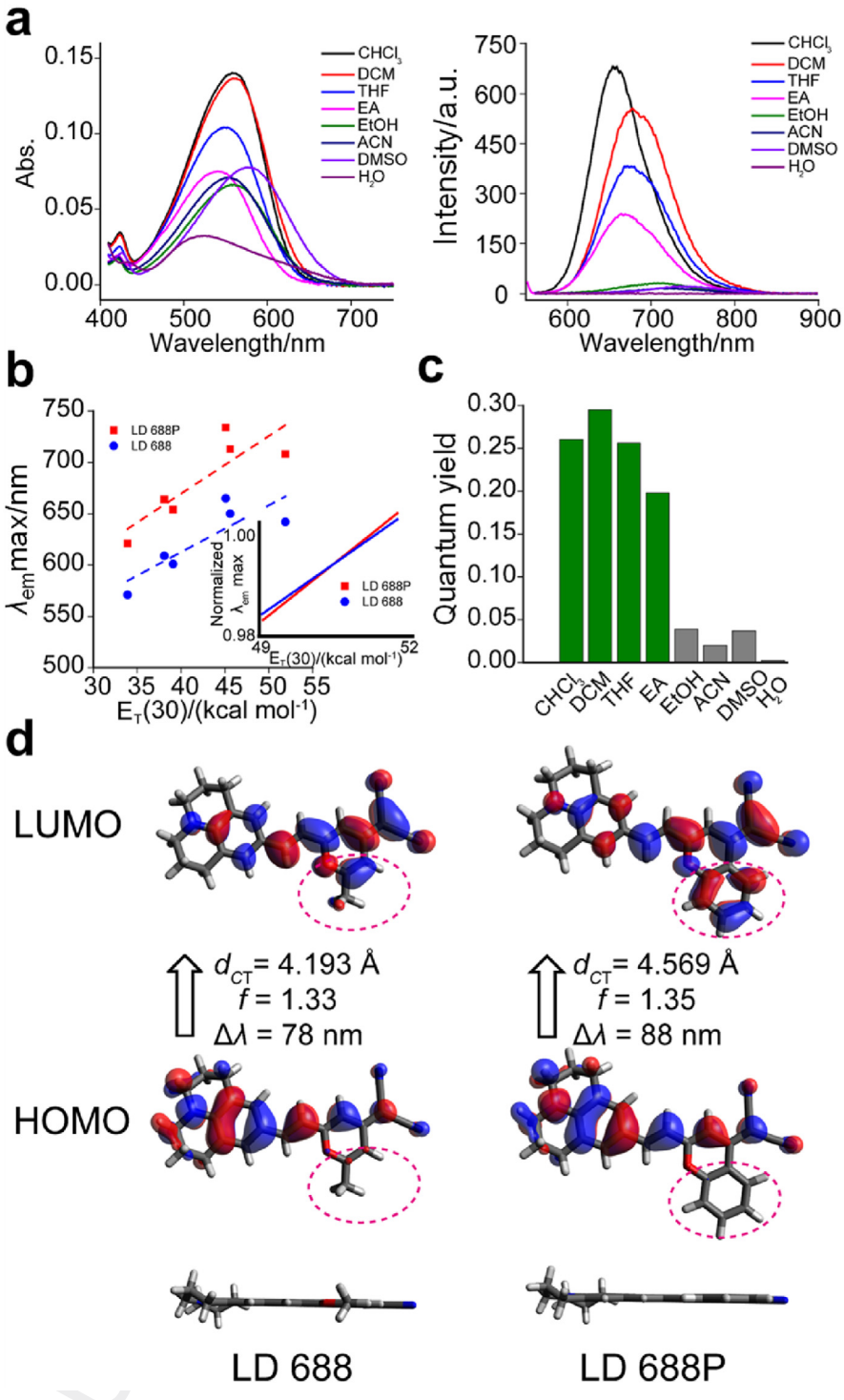

Fig. 2. (a) Absorption and fluorescence Spectra of LD 688P (5 μM) in solvents of different polarity. (b) Fitted curve of the maximum of emission wavelength of LD 688 *vs.* solvent polarity parameters: E_T (30). Inset: Fitted curve of the normalized emission wavelength maximum *vs.* E_T (30). (c) Quantum yields of LD 688P in diverse solvents. (d) Optimized molecular of LD 688 and LD 688P in S_0, and the corresponding HOMO and LUMO distribution in S_1.

was also clearly observed that LD 688P displayed noteworthy strong emissions in the solvents with weak polarity and high hydrophobicity (DCM: $\phi = 0.29$), almost no fluorescence emission in water ($\phi = 0.002$) (Fig. 2a and c and Table S2), enabling the desired fluorogenic properties of the probe.

For making further efforts to understand the spectral properties of LD 688 and LD688P, we compare the electronic configuration properties of the ground and excited state for both LD 688 and LD 688P employing quantum chemistry calculations. These two compounds displayed fine planar structure and showed significant charge transfer in the excited state. Particularly, the electron density of the conjugated system adjacent to the acceptor.

(the red dotted circle region) changed drastically, which showed no electron delocalization in the ground state, but the opposite in the excited state. It was the introduction of the benzene ring that expanded the electron delocalization system of the molecule in the excited state,

producing a large wavelength red shift. Further, the CT distance (d_{CT}) [32] used to evaluate the degree of intramolecular charge transfer (ICT) was obtained. It was observed that the d_{CT} of LD 688P (4.569 Å) was larger than that of LD 688 (4.193 Å), with a larger Stokes shift (Δλ), revealing that LD 688P showed a more significant ICT character. In addition, LD 688P exhibited greater oscillator strength(*f*). These results suggest that LD 688P is more prominent than LD 688 in some aspects such as the degree of ICT.

Based on the above photophysical properties of LD 688P, we expect it can be used for wash free imaging of living cells. Firstly, we performed co-staining experiments on LDs in living HeLa cells (Fig. 3a). The cells were incubated with LD 688P and BODIPY 493 for 30 min, and then the pictures were recorded under confocal fluorescence microscopy without the washing steps. Strong fluorescence was observed from LD 688P with negligible background interference and the fluorescence from which can be overlapped with BODIPY 493 with a Pearson's R value as high as 0.96. We attribute this low-background imaging to two major reasons: one is that LD 688P possesses suitable lipid solubility with a Clog *P* value of 5.4, which is very selective for lipid droplets [30]. Another is that the excellent environmental sensitivity of LD 688P plays a key role. The fluorescence of LD 688P only turns on in the weakly polar and aprotic microenvironment like LDs, avoiding the interference of imaging background caused by non-specific staining.

Before conducting the following experiments, we investigated the biocompatibility of LD 688P. From the MTT experimental results (Fig. S4) we found that ˃ 90% of HeLa cells survived after 24 h (20 μM LD 688P incubation), demonstrating the low toxicity of LD 688P towards cultured cell lines, ensuring that LD 688P is a suitable LD probe for imaging of living cells.

To investigate the fluorescence properties of LD 688P in LDs, the spectra *in situ* were collected. It can be observed that different regions exhibit the same spectra (Fig. 3b), with a maximum emission wavelength of approximately 620 nm, indicating that LD 688P is a red-emitting LD-dye.

To enable long-term observation of LD dynamics, the photostability of LD-dyes is critical. Especially for red-emitting dyes, photobleaching is particularly severe because flexible conjugated chains are easily attacked by singlet oxygen. Therefore, we explored the stability of LD 688P under confocal fluorescence microscopy. The photostability of LD 688P was evaluated by the repeated acquisition of confocal images in the identical region (Fig. 4). The HeLa cells were incubated with LD 688P (1 μM) for 1 h before imaging. It was observed that LD 688P displayed good photostability under the excitation of a 543 nm laser. After continuous imaging, the fluorescence intensity of the probe remains about 80% of its initial intensity. On the contrary, the commercial dye LD 540 is quickly bleached (Fig. S5). It could be observed that the LDs in the enlarged area were still clearly visible after continuous imaging, ensuring that LD 688P has the potential to observe LD dynamics for a long time. We speculated the introduction of a rigid benzene ring increased the stability of the dye while increasing the wavelength.

LDs are highly dynamic cellular organelles whose size reflects the ability of adipose tissue to store lipids and is closely related to the occurrence of metabolic diseases such as obesity, diabetes, and fatty liver [33,34]. Fusion of LDs regulated by various factors will increase LD size, which can reveal new physiological functions of LDs. The above results show that LD 688P is a highly selective and photostable LD-dye. Then we use LD 688P for SIM imaging to observe the interaction between LDs in real time. LDs are widely distributed in cells, and we accidently observe that LDs have large clusters at the pole of the cell, and small clusters of LDs are distributed in the middle of cells. For these two phenomena with significantly different numbers of LDs, we performed long-term imaging. In a region with large clusters of LDs, multiple fusion processes of LDs were observed accompanied by LD enlargement and an increase in LD brightness (Fig. 5a, Movie S1). The diameter of an LD increased by nearly four times through five fusions with adjacent LDs (Fig. 5b). Similarly, in the area of small clusters of LDs, LDs also undergo multiple fusions. Interestingly, a seemingly regular phenomenon that two LDs fused with adjacent LDs in a centrosymmetric manner was observed (Fig. 5c, Movie

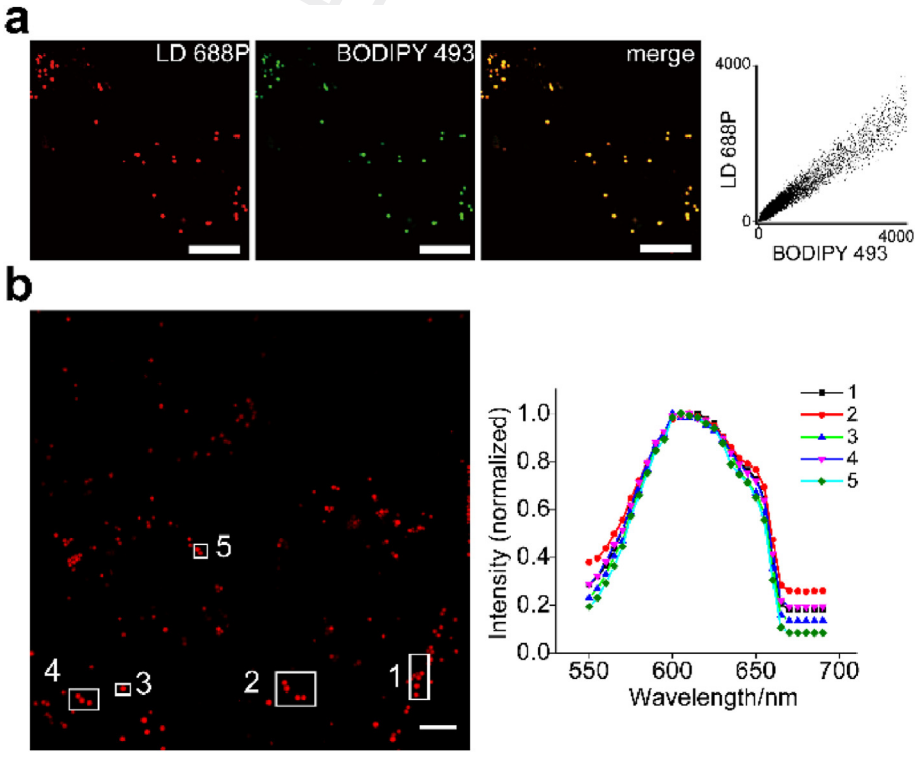

Fig. 3. (a) Confocal imaging of HeLa cells stained with LD 688P (1 μM) and BODIPY 493 (0.5 μM) and the Pearson's coefficient. Scale bar: 10 μm. (b) *In situ* spectroscopy of LD 688P in LDs plot by multiple regions. Scale bar: 10 μm.

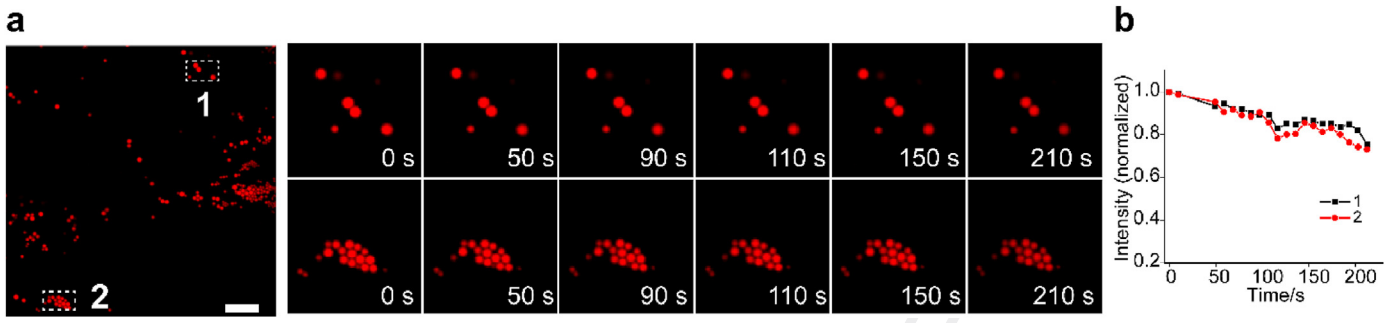

Fig. 4. (a) Confocal images of LDs stained with LD 688P (1 μM) within 210 s. Scale bar: 10 μm. (b) Relative fluorescence intensity changes of enlarged region in living HeLa (under 70% 543 nm laser).

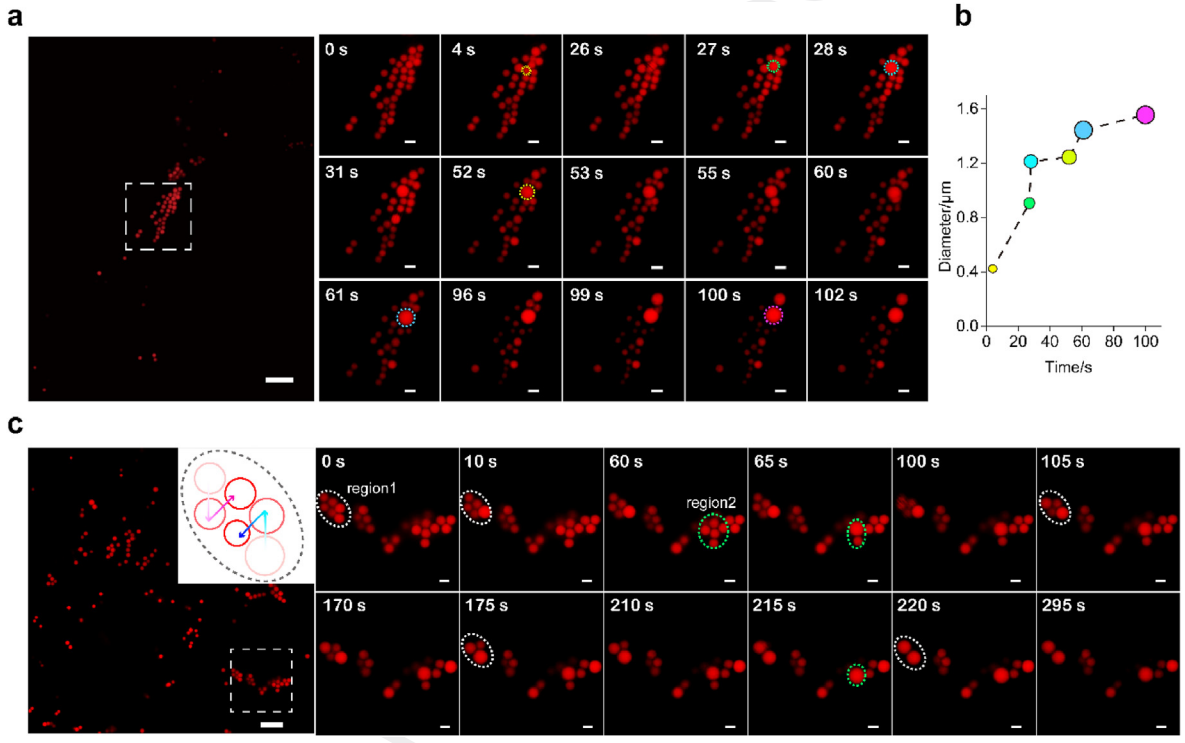

Fig. 5. SIM imaging of LD 688P (1 μM) in living HeLa. (a)SIM imaging of multiple fusions of LDs. Scale bar: 5 μm. (Scale bar for enlarged images: 1 μm) (b) Plot of lipid droplet diameter *vs*. time during fusion. (c) SIM imaging of fusions of LDs in a centrosymmetric manner. A simple schematic diagram was in the inset. Scale bar: 5 μm. (Scale bar for enlarged images: 1 μm).

S2). In region 1, the six LDs gathered together to form a parallelepiped. Over time, the two LDs in the lower right corner and the upper left corner fused twice according to the route shown in the inset of the figure, implying that the fusion of LDs may have a specific orientation. In addition, four LDs fused almost simultaneously within 5 s and were observed in region 2, which indicated that the fusion rate of LDs was extremely fast and required high temporal resolution of the LDs imaging.

Supplementary data related to this article can be found at https://doi.org/10.1016/j.gce.2022.07.002.

In conclusion, we have developed a strategy to construct long wavelength D-π-A-π type LD-dyes, modifying commercial dye LD 688 to obtain LD 688P, in which the incorporated benzene ring increased the wavelength by delocalization of electrons in the excited state. Compared with LD 688, the maximum emission wavelength of LD 688P was red-shifted by 53 nm. Additionally, LD 688P proved to be highly selective and photostable for tracing LD dynamics by super-resolution microscopy. The phenomenon of multiple consecutive fusions and fusions in a centrosymmetric manner was observed. We believe that this strategy provides an option for the construction of longer emission dyes.

Declaration of competing interest

The authors declare that they have no known competing financial interests or personal relationships that could have appeared to influence the work reported in this paper.

Acknowledgments

This work is supported by the National Natural Science Foundation of China (22078314, 21878286, 21908216) and Dalian Institute of Chemical Physics (DICPI202142, DICPI201938, and DICPZZBS201805). The authors thank the support from A*STAR under its Advanced Manufacturing and Engineering Program (A2083c0051), the Ministry of Education, Singapore (MOE-MOET2EP10120-0007).

Appendix A. Supplementary data

Supplementary data to this article can be found online at https://doi.org/10.1016/j.gce.2022.07.002.

References

[1] R.V. Farese Jr., T.C. Walther, Lipid droplets finally get a little R-E-S-P-E-C-T, Cell 139 (2009) 855–860.
[2] A.R. Thiam, R.V. Farese Jr., T.C. Walther, The biophysics and cell biology of lipid droplets, Nat. Rev. Mol. Cell Biol. 14 (2013) 775–786.
[3] A. Sathyanarayan, M.T. Mashek, D.G. Mashek, ATGL promotes autophagy/lipophagy *via* SIRT1 to control hepatic lipid droplet catabolism, Cell Rep. 19 (2017) 1–9.
[4] T.C. Walther, R.V. Farese Jr., Lipid droplets and cellular lipid metabolism, Annu. Rev. Biochem. 81 (2012) 687–714.
[5] A.M. Valm, S. Cohen, W.R. Legant, J. Melunis, U. Hershberg, E. Wait, A.R. Cohen, M.W. Davidson, E. Betzig, J. Lippincott-Schwartz, Applying systems-level spectral imaging and analysis to reveal the organelle interactome, Nature 546 (2017) 162–166.
[6] J.A. Olzmann, P. Carvalho, Dynamics and functions of lipid droplets, Nat. Rev. Mol. Cell Biol. 20 (2019) 137–155.
[7] J.K. Zehmer, Y. Huang, G. Peng, J. Pu, R.G. Anderson, P. Liu, A role for lipid droplets in inter-membrane lipid traffic, Proteomics 9 (2009) 914–921.
[8] M. Konige, H. Wang, C. Sztalryd, Role of adipose specific lipid droplet proteins in maintaining whole body energy homeostasis, Biochim. Biophys. Acta 1842 (2014) 393–401.
[9] N. Krahmer, R.V. Farese Jr., T.C. Walther, Balancing the fat: lipid droplets and human disease, EMBO Mol. Med. 5 (2013) 973–983.
[10] F. Li, X. Lan, X.J. Liang, Intracellular aggregations of biological elements: from simple to complex, Aggregate 2 (2021) e27.
[11] H. Cao, Y. Yang, J. Li, AIEgen–lipid structures: assembly and biological applications, Aggregate 1 (2020) 69–79.
[12] X. Huang, J. Fan, L. Li, H. Liu, R. Wu, Y. Wu, L. Wei, H. Mao, A. Lal, P. Xi, L. Tang, Y. Zhang, Y. Liu, S. Tan, L. Chen, Fast, long-term, super-resolution imaging with Hessian structured illumination microscopy, Nat. Biotechnol. 36 (2018) 451–459.
[13] Y. Guo, D. Li, S. Zhang, Y. Yang, J.J. Liu, X. Wang, C. Liu, D.E. Milkie, R.P. Moore, U.S. Tulu, D.P. Kiehart, J. Hu, J. Lippincott-Schwartz, E. Betzig, D. Li, Visualizing intracellular organelle and cytoskeletal interactions at nanoscale resolution on millisecond timescales, Cell 175 (2018) 1430–1442.
[14] W. Zhang, L. Xu, L. Zhu, Y. Liu, S. Yang, M. Zhao, Lipid droplets, the central hub integrating cell metabolism and the immune system, Front. Physiol. 12 (2021), 746749.
[15] A.S. Klymchenko, Solvatochromic and fluorogenic dyes as environment-sensitive probes: design and biological applications, Acc. Chem. Res. 50 (2017) 366–375.
[16] R. Zhou, C. Wang, X. Liang, F. Liu, X. Yan, X. Liu, P. Sun, H. Zhang, Y. Wang, G. Lu, Stimulated emission depletion (STED) super-resolution imaging with an advanced organic fluorescent probe: visualizing the cellular lipid droplets at the unprecedented nanoscale resolution, ACS Mater. Lett. 3 (2021) 516–524.
[17] M. Taki, K. Kajiwara, E. Yamaguchi, Y. Sato, S. Yamaguchi, Fused thiophene-S,S-dioxide-based super-photostable fluorescent marker for lipid droplets, ACS Mater. Lett. 3 (2020) 42–49.
[18] H. Chen, B. Dong, Y. Tang, W. Lin, A unique "integration" strategy for the rational design of optically tunable near-infrared fluorophores, Acc. Chem. Res. 50 (2017) 1410–1422.
[19] L. Yuan, W. Lin, S. Zhao, W. Gao, B. Chen, L. He, S. Zhu, A unique approach to development of near-infrared fluorescent sensors for *in vivo* imaging, J. Am. Chem. Soc. 134 (2012) 13510–13523.
[20] M.-Y. Wu, J.-K. Leung, C. Kam, T.Y. Chou, D. Wang, S. Feng, S. Chen, A near-infrared AIE probe for super-resolution imaging and nuclear lipid droplet dynamic study, Mater. Chem. Front. 5 (2021) 3043.
[21] H. Tian, A.C. Sedgwick, H.-H. Han, S. Sen, G.-R. Chen, Y. Zang, J.L. Sessler, T.D. James, J. Li, X.-P. He, Fluorescent probes for the imaging of lipid droplets in live cells, Coord. Chem. Rev. 427 (2021), 213577.
[22] C.W. Song, U. Tamima, Y.J. Reo, M. Dai, S. Sarkar, K.H. Ahn, A rationally designed polarity-viscosity sensitive probe for imaging lipid droplets, Dyes Pigments 171 (2019), 107718.
[23] T.K. Fam, A.S. Klymchenko, M. Collot, Recent advances in fluorescent probes for lipid droplets, Materials 11 (2018) 1768.
[24] M. Kang, X. Gu, R.T. Kwok, C.W. Leung, J.W. Lam, F. Li, B.Z. Tang, A near-infrared AIEgen for specific imaging of lipid droplets, Chem. Commun. 52 (2016) 5957–5960.
[25] Y. Tatenaka, H. Kato, M. Ishiyama, K. Sasamoto, M. Shiga, H. Nishitoh, Y. Ueno, Monitoring lipid droplet dynamics in living cells by using fluorescent probes, Biochemistry 58 (2019) 499–503.
[26] M. Collot, T.K. Fam, P. Ashokkumar, O. Faklaris, T. Galli, L. Danglot, A.S. Klymchenko, Ultrabright and fluorogenic probes for multicolor imaging and tracking of lipid droplets in cells and tissues, J. Am. Chem. Soc. 140 (2018) 5401–5411.
[27] B. Lu, J. Yin, C. Liu, W. Lin, NIR fluorescence imaging of lipid drops viscosity in liver organs of diabetic mice, Dyes Pigments 187 (2021), 109120.
[28] X. Zhang, L. Yuan, J. Jiang, J. Hu, A. du Rietz, H. Cao, R. Zhang, X. Tian, F. Zhang, Y. Ma, Z. Zhang, K. Uvdal, Z. Hu, Light-up lipid droplets dynamic behaviors using a red-emitting fluorogenic probe, Anal. Chem. 92 (2020) 3613–3619.
[29] D. Wang, H. Su, R.T.K. Kwok, G. Shan, A.C.S. Leung, M.M.S. Lee, H.H.Y. Sung, I.D. Williams, J.W.Y. Lam, B.Z. Tang, Facile synthesis of red/NIR AIE luminogens with simple structures, bright emissions, and high photostabilities, and their applications for specific imaging of lipid droplets and image-guided photodynamic Therapy, Adv. Funct. Mater. 27 (2017), 1704039.
[30] J. Chen, C. Wang, W. Liu, Q. Qiao, H. Qi, W. Zhou, N. Xu, J. Li, H. Piao, D. Tan, X. Liu, Z. Xu, Stable super-resolution imaging of lipid droplet dynamics through a buffer strategy with a hydrogen-bond sensitive fluorogenic probe, Angew Chem. Int. Ed. Engl. 60 (2021) 25104–25113.
[31] K.S. Levchenko, K.A. Chudov, E.V. Zinoviev, K.A. Lyssenko, A.N. Fakhrutdinov, D.U. Demin, N.O. Poroshin, P.S. Shmelin, E.P. Grebennikov, Synthesis of unsymmetrical 2-(2-vinyl-4H-chromen-4-ylidene)malononitrile dyes *via* Knoevenagel reaction, Tetrahedron Lett. 60 (2019) 1505–1508.
[32] C.A. Guido, P. Cortona, B. Mennucci, C. Adamo, On the metric of charge transfer molecular excitations: a simple chemical descriptor, J. Chem. Theor. Comput. 9 (2013) 3118–3126.
[33] F. Boschi, V. Rizzatti, M. Zamboni, A. Sbarbati, Lipid droplets fusion in adipocyte differentiated 3T3-L1 cells: a Monte Carlo simulation, Exp. Cell Res. 321 (2014) 201–208.
[34] J. Marschallinger, T. Iram, M. Zardeneta, S.E. Lee, B. Lehallier, M.S. Haney, J.V. Pluvinage, V. Mathur, O. Hahn, D.W. Morgens, J. Kim, J. Tevini, T.K. Felder, H. Wolinski, C.R. Bertozzi, M.C. Bassik, L. Aigner, T. Wyss-Coray, Lipid-droplet-accumulating microglia represent a dysfunctional and proinflammatory state in the aging brain, Nat. Neurosci. 23 (2020) 194–208.